3562 *Inorg. Chem.* **1985**, *24*, 3562-3567

Contribution from the Department of Chemistry,
Concordia University, Montreal, Quebec H3G 1M8, Canada

Photoelectrochemical Studies of Maleonitriledithiolate Complexes of Nickel, Palladium, Platinum, and Copper

LALCHAN PERSAUD and COOPER H. LANGFORD*

Received November 14, 1984

The spectroscopic and electrochemical behavior of bis(maleonitriledithiolate) (mnt) complexes of Ni, Pd, Pt, and Cu have been compared at Pt and transparent SnO_2 electrodes. There were no major qualitative differences, but there was evidence that heterogeneous electron transfer was slower at SnO_2. The transparent electrodes were exploited for photoelectrochemistry with visible light. For $M(mnt)_2^{2-}$, where M = Ni, Pt, the main visible band corresponds to MLCT excitation and cathodic photocurrents were observed. For M = Pd, the corresponding band is assigned LMCT and no current was observed. In the case of M = Cu, no current was observed for the MLCT band of the odd-electron 2− complex but an anodic current was observed for the 3− reduced form. All currents were small (nA) and in phase with the chopper. Estimation of the competition between diffusion to the electrode (for reaction) and relaxation of the excited state suggests excited-state lifetimes in the short nanosecond time domain.

Introduction

The family of complexes represented by structure I (M = Ni, Pd, Pt, Cu) presents interesting prospects for electron-transfer photochemistry because the charge, *n*, may take on values from 0 to 3− with little change in structure and the complexes are strongly colored. In this respect, they are in a distant sense suggestive of the porphyrins. Moreover, E_0 values cover a significant range.

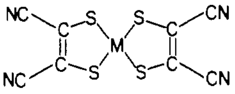

I

Two kinds of photoreactivity for these complexes have been reported. In the UV, members of the family have been shown to initiate hydrogen evolution from solvents, probably by charge transfer to solvent types of excitation.[1,2] In the nearer UV, photooxidation of chlorocarbon solvents is observed.[3] So far, no reactions have been observed upon irradiation of the bands in the visible or red. Perhaps the reason has been the lack of a suitable partner for photochemical reactivity at lower energies. In our laboratories, a technique for detecting photochemical electron-transfer reactivity has been developed that used irradiation through an optically transparent electrode to provide the electrode as a reaction partner having a variable free energy for the reactions with the excited states. In the case of the tris(bipyridine)iron(II) complex, this technique allowed detection of electron transfer from a 1-ns-lifetime excited state.[4] We have used this technique to explore possible reactions of the maleonitrile complexes under irradiation in the visible region.

Experimental Section

Solvents, simple salts, iodine, and potassium tetrachloroplatinate were reagent grade materials from well-known suppliers and were used as received. In the course of synthetic work, deoxygenations were carried out by bubbling purified nitrogen. Water was distilled in glass. Microanalyses were by Galbraith Laboratories, Knoxville, TN.

Sodium maleonitriledithiolate (Na_2mnt) was prepared by a modification of the dicyanodithioformate procedure of Bahr and Schleitzer.[5] A 5-g sample of powdered NaCN was added to 12 mL of CS_2. The mixture was stirred for 16 h until a red-black mass of sodium dithioformate was obtained. This was recrystallized from 1:1 isobutyl and isopropyl alcohol. The mnt dianion was then obtained by spontaneous dimerization in chloroform for 7 days. Purification was effected by recrystallization from methanol/ether. The yellow product was stored in the dark at 5 °C.

$[(C_2H_5)_4N]_2[Ni(mnt)_2]$. The well-known 2−oxidation level Ni complex of mnt (formally Ni(II) was prepared according to a published procedure,[6] purified by recrystallization from water–acetone several times, and confirmed by comparison of the UV–vis spectra with literature reports.[7] $[(C_2H_5)_4N]_2[Cu(mnt)_2]$, the related Cu complex, formally Cu(II), was prepared similarly. A deaerated alcohol solution of $CuCl_2$ was added to one of Na_2mnt was vigorous stirring. (It is important to use an excess of ligand in order to avoid a thick sludge.) Shiny dark red crystals separate. They were recrystallized from acetonitrile–water. Anal. Calcd for $[(C_2H_5)_4N]_2[CuS_4C_4(CN)_4]$: C, 47.69; H, 6.67; N, 13.90; S, 21.22; Cu, 10.51. Found: C, 47.45; H, 6.82; N, 13.84; S, 21.06; Cu, 10.46.

$[(C_2H_5)_4N]_2[Pt(mnt)_2]$ and $[(C_2H_5)_4N]_2[Pd(mnt)_2]$. These were synthesized by the method of Benson et al.[8] and recrystallized from ethanol–water. The Pd complex spectrum was compared to literature spectra.[7] The Pt complex was analyzed. Anal. Calcd for $[(C_2H_5)_4N]_2[Pt(mnt)_2]$: C, 39.17; H, 5.48; N, 11.42; S, 17.43; Pt, 26.51. Found: C, 38.82; H, 5.27; N, 11.32; S, 17.69; Pt, 26.31.

The oxidized complexes, $[M(mnt)_2]^-$, were prepared as follows. For $[(C_2H_5)_4N][Ni(mnt)_2]$, the iodine oxidation as described by Davison et al.[9] was used. The product spectrum did not agree with some literature reports in that no 366-nm band was found. Investigation revealed that this band appears to have arisen from excess I_2 remaining. Anal. Calcd for $[(C_2H_5)_4N][Ni(mnt)_2]$: C, 40.95; H, 4.30; N, 14.92; S, 27.32; N, 12.51. Found: C, 41.10; H, 4.33; N, 14.90; S, 27.29; Ni, 12.40. $[(C_2H_5)_4N][Pd(mnt)_2]$ was obtained by the published procedure.[9] $[(C_2H_5)_4N][Cu(mnt)_2]$ was prepared by ferric perchlorate oxidation of $Cu(mnt)_2^{2-}$ in CH_3CN. The product was precipitated on addition of water and then recrystallized from CH_2Cl_2–ethanol with cooling to −10 °C. Anal. Calcd for $[(C_2H_5)_4N][Pd(mnt)_2]$: C, 37.17; H, 3.90; N, 13.54; S, 24.81; Pd, 20.58. Found: C, 37.36; H, 4.03; N, 13.37; S, 24.89; Pd, 20.38. Anal. Calcd for $[(C_2H_5)_4N][Cu(mnt)_2]$: C, 40.53; H, 4.25; N, 14.77; S, 27.05. Found: C, 40.25; H, 4.33; N, 14.17; S, 27.35.

The UV–vis spectra of these complexes are collected in Tables I and II.

Electrochemical Measurements. Dc cyclic voltammetric experiments were performed with a PAR 363 potentiostat in conjunction with a locally constructed triangular pulse generator based on a design in the literature.[10] Measurements were made at a Pt wire and also at SnO_2 working electrodes. The SnO_2 electrodes were the same type used for photoelectrochemical measurements and were subjected to the same treatment prior to usage in the CH_3CN medium. Reference electrodes were either AgCl (saturated KCl) separated from the voltammetric cell by a fine-frit tube containing the appropriate depolarizer solution or Ag/Ag^+ (0.1 M $AgNO_3$) in CH_3CN, a redox couple that was found to be at +0.27 V vs. the external Ag/AgCl (saturated KCl). A Pt-wire auxiliary electrode was used. Measurements were performed in Spectrograde acetonitrile (American Chemicals) with 0.1 M anhydrous sodium perchlorate (Anachemia) as supporting inert electrolyte unless otherwise noted. Reactants were dissolved directly inside the cell, and the sample solutions were degassed by bubbling of prepurified N_2.

Photoelectrochemical Measurements. All photoelectrochemical experiments were performed at optically transparent electrodes with a

---

(1) H. Rainer, W. Schlumann, and H. Kisch, *Angew. Chem.* **19**, 645 (1980).

(2) A. Vogler and H. Kunkley, *Inorg. Chem.*, **21**, 1172 (1982).

(3) D. M. Dooley and B. M. Patterson, *Inorg. Chem.* **21**, 4330 (1982).

(4) J. Phillips, J. A. Koningstein, and C. H. Langford, *J. Chem. Soc., Chem. Commun.*, 425 (1977).

(5) G. Bahr and G. Schleitzer, *Chem. Ber.*, **90**, 438 (1957).

(6) E. Billig, R. Williams, I. Bernal, J. H. Walters, and H. B. Gray, *Inorg. Chem.*, **2**, 663 (1964).

(7) S. I. Shupack, E. Billig, R. J. H. Clark, R. Williams, and H. B. Gray, *J. Am. Chem. Soc.*, **86**, 4594 (1964).

(8) R. E. Benson, L. R. Melby, and J. F. Weiher, *J. Am. Chem. Soc.*, **86**, 4329 (1964).

(9) A. Davison, N. Edelstein, R. H. Holm, and H. Maki, *Inorg. Chem.*, **2**, 1227 (1963).

(10) C. G. Pablo, Chem., *Biomed. Environ. Instrum.* **10**, 197 (1980).

0020-1669/85/1324-3562$01.50/0

Table I. Electronic Absorption Spectra of $M(mnt)_2^n$ Complexes in Acetonitrile Solutions

complex	V/cm^{-1}	wavelength/nm[d]	ϵ/dm^3 M^{-1} cm^{-1}	assignts *a*	assignts *b*
$Ni(mnt)_2^{2-}$	11 690	855	30	$^1A_g \rightarrow {}^1B_{1g}\ (x^2 - y^2 \rightarrow xy)$	*c*
	17 500	571	570	$^1A_g \rightarrow {}^1B_{3g}\ (xz \rightarrow xy)$	$^1A_g \rightarrow {}^1B_{2u}, {}^1B_{3u}\ (N{=}S \rightarrow M)$
	19 250	519	1 250	$^1A_g \rightarrow {}^1A_u\ (x^2 - y^2 \rightarrow L\pi^*)$	$^1A_g \rightarrow {}^1B_{1g}\ (N{=}S \rightarrow M)$
	21 000	476	3 800	$^1A_g \rightarrow {}^1B_{2u}\ (xz \rightarrow L\pi^*)$	*c*
	26 400	378	6 600	$^1A_g \rightarrow {}^1B_{2u}, {}^1B_{3u}\ (L\pi \rightarrow xy)$	*c*
	31 300	319	30 000	$^1A_g \rightarrow {}^1B_{2u}\ (L\pi \rightarrow L\pi^*)$	*c*
	37 000	270	50 000	$^1A_g \rightarrow {}^1B_{2u}, {}^1B_{3u}\ (L\sigma \rightarrow xy)$	
$Pd(mnt)_2^{2-}$	15 700	637	64	$^1A_g \rightarrow {}^1B_{1g}\ (x^2 - y^2 \rightarrow xy)$	$^1A_g \rightarrow {}^1B_{1g}\ (x^2 - y^2 \rightarrow xy)$
	22 700	440	5 700	$^1A_g \rightarrow {}^1B_{2u}, {}^1B_{3u}\ (L\pi \rightarrow xy)$	$^1A_g \rightarrow {}^1B_{1g}\ (N{=}S \rightarrow M)$
	25 800	387	2 840	$^1A_g \rightarrow {}^1A_u\ (x^2 - y^2 \rightarrow L\pi^*)$	*c*
	30 800	325	20 200	$^1A_g \rightarrow {}^1B_{2u}\ (L\pi \rightarrow L\pi^*)$	*c*
	33 900	295	47 000	$^1A_g \rightarrow {}^1B_{2u}, {}^1B_{3u}\ (L\sigma \rightarrow xy)$	*c*
	37 800	266	45 000	*c*	*c*
	42 800	234	42 800	*c*	*c*
$Pt(mnt)_2^{2-}$	14 410	694	49	$^1A_g \rightarrow {}^3B_{1g}\ (x^2 - y^2 \rightarrow xy)$	*c*
	15 650	639	56	$^1A_g \rightarrow {}^3B_{3g}\ (xz \rightarrow xy)$	*c*
	18 500	540	1 220	$^1A_g \rightarrow {}^1B_{1g}\ (x^2 - y^2 \rightarrow xy)$	
				$^1A_g \rightarrow {}^1A_u\ (x^2 - y^2 \rightarrow L\pi^*)$	*c*
$Pt(mnt)_2^{2-}$	21 100	473	3 470	$^1A_g \rightarrow {}^1B_{2u}\ (xz \rightarrow L\pi^*)$	*c*
	29 700	336	15 600	$^1A_g \rightarrow {}^1B_{2u}\ (L\pi \rightarrow L\pi^*)$	*c*
	32 300	309	13 400	$^1A_g \rightarrow {}^1B_{2u}, {}^1B_{3u}\ (L\pi \rightarrow L\pi^*)$	*c*
	38 500	260	17 000	*c*	*c*
	43 800	228	43 500	$^1A_g \rightarrow {}^1B_{2u}, {}^1B_{3u}\ (L\sigma \rightarrow xy)$	*c*
$Ni(mnt)_2^-$	8 330	1200[d]	329[d]	$4b_{2g} \rightarrow 4a_g\ (xz \rightarrow x^2 - y^2)$	$4a_g \rightarrow 3b_{2g}\ (M \rightarrow \pi)$
	11 790	848[d]	8 000[d]	$3b_{1u}, 2b_{2u}, 2b_{3u} \rightarrow 4a_g\ (L\pi \rightarrow x^2 - y^2)$	$2b_{3g} \rightarrow 3b_{2g}\ (M \rightarrow \pi)$
	16 666	600	668[f]	$3b_{3g} \rightarrow 4a_g$	$2b_{1u} \rightarrow 3b_{1g}\ (\pi \rightarrow M)$
	18 349	545[e]	798[f]	$3a_g \rightarrow 4a_g$	$N{=}S{:} \rightarrow 3b_{2g}\ (N{=}S{:} \rightarrow \pi)$ $N{=}S{:} \rightarrow 3b_{1g}\ (N{=}S{:} \rightarrow \pi)$
	20 694	477	2 490[f]	$1b_{2u}, 1b_{3u} \rightarrow 4a_g\ (L\sigma \rightarrow x^2 - y^2)$	$3b_{2g} \rightarrow 2a_u\ (\pi \rightarrow \pi)$ $2a_g \rightarrow 3b_{1g}\ (N{=}S{:} \rightarrow M)$
	27 027	370[e]	7 114[f]	$2b_{3u}, 2b_{2u} \rightarrow 3b_{1g}\ (L\pi \rightarrow xy)$	$2b_{3g} \rightarrow 2a_u\ (M \rightarrow \pi)$
	32 154	311	33 873[f]	$3b_{1u} \rightarrow 4b_{3g}\ (L\pi \rightarrow L\pi^*)$	$1a_u \rightarrow 3b_{2g}\ (\pi \rightarrow \pi)$
	37 037	270	34 017[f]	$1b_{3u}, 1b_{2u} \rightarrow 3b_{1g}\ (L\sigma \rightarrow xy)$	*c*
	43 478	230	19 093[f]	*c*	*c*

[a] Given in ref 7. [b] Given in ref 16. [c] Not assigned. [d] Calculated from frequency (cm^{-1}) values of ref 7 and 19. [e] Shoulder. [f] Peak maximum and ϵ values are from this study.

Table II. Electronic Absorption Spectra of $M(mnt)_2^n$ Complexes in Acetonitrile Solutions

complex	V/cm^{-1}	wavelength/nm	ϵ/dm^3 M^{-1} cm^{-1}	assignts
$Cu(mnt)_2^{2-}$	8 299	1205[a]	94	$4a_g \rightarrow 3b_{1g}\ (x^2 - y^2 \rightarrow xy)$
	21 097	474	4 537	$4b_{2g} \rightarrow 3a_u\ (xz \rightarrow L\pi^*)$
	23 256	430[b]	4 764	$2b_{3u}, 2b_{2u} \rightarrow 3b_{1g}\ (L\pi \rightarrow xy)$
	27 174	368	10 549	$3b_{3g}, 3a_g \rightarrow 3b_{1g}$
	28 736	348	10 501	$3b_{2g}, 2a_g \rightarrow 3b_{1g}$
	31 546	317	15 670	$3b_{1u} \rightarrow 4b_{3g}\ (L\pi \rightarrow L\pi^*)$
	35 842	279	23 156	$1b_{3u}, 1b_{2u} \rightarrow 3b_{1g}\ (L\sigma \rightarrow xy)$
	44 053	227	20 000	
$Cu(mnt)_2^-$	6 400	1563[a]	337	$4a_g \rightarrow 3b_{1g}\ (x^2 - y^2 \rightarrow xy)$
	13 000	769[a]	110	$4b_{2g} \rightarrow 3b_{1g}\ (xz \rightarrow xy)$
	19 531	512[b]	1 159	$4a_g \rightarrow 3a_u\ (x^2 - y^2 \rightarrow L\pi^*)$
	25 773	388[c]	16 477	$2b_{3u}, 2b_{2u} \rightarrow 3b_{1g}\ (L\pi \rightarrow xy)$
	31 250	320	9 364	$3b_{1u} \rightarrow 4b_{3g}\ (L\pi \rightarrow L\pi^*)$
	35 211	284	20 566	$3b_{3g} \rightarrow 4b_{3g}, 3a_u$
	37 037	270	21 911	$1b_{2u}, 1b_{3u} \rightarrow 3b_{1g}\ (L\sigma \rightarrow xy)$
$Pd(mnt)_2^-$	15 314	653	472	$4a_g \rightarrow 3b_{1g}\ (x^2 - y^2 \rightarrow xy)$
	16 950	590[b]	580	$3b_{3g} \rightarrow 4a_g$
	18 382	544[b]	951	$3a_g \rightarrow 4a_g$
	20 704	483[c]	2 672	$4b_{2g} \rightarrow 3a_u, 4b_{3g}\ (xz \rightarrow L\pi^*)$
	28 818	347[b]	5 491	$3b_{1u} \rightarrow 4b_{3g}\ (L\pi \rightarrow L\pi^*)$
	36 496	274	45 000	$1b_{3u}, 1b_{2u} \rightarrow 3b_{1g}\ (L\sigma \rightarrow xy)$
	43 478	230	22 000	
	9 000	1111[a]	13 800	$3b_{1u}, 2b_{2u}, 2b_{3u} \rightarrow 4a_g\ (L\pi \rightarrow x^2 - y^2)$

[a] Calculated from frequency (cm^{-1}) values of ref 9, 18, and 19. [b] Shoulder. [c] Broad band probably contains two electronic transitions.

usable window of 360 to 600 nm. These electrodes were fabricated as disks 2.5 cm in diameter from Corning's SnO_2-coated "NESA" glass obtained from O.H. Johns Glass Division and marketed as IR reflective conducting glass. Typical resistances are less than 50 Ω. The electrodes were prepared for use by soaking in absolute ethanol at 70 °C for 6 h and then washed several times with hot absolute ethanol and dried acetonitrile. They were stored under vacuum at 160–180 °C prior to use. Heating was continued for at least 12 h. Measurements were conducted in a Teflon flow cell equipped with a Pt-coil counter electrode and an Ag/Ag^+ (0.1 M $AgNO_3$ in CH_3CN) reference electrode. The optically transparent electrode was tightly pressed against a silicone rubber "O" ring and a thin brass ring in the wall of the cell. It was held securely in this position from the outside by means of screws and a brass plate that permitted an optical window of 0.78 cm^2. The "O" ring served as a seal and prevented electrolytic solution from coming in contact with the brass ring on the outer periphery of the SnO_2 electrode. The brass ring provided the electrical connection between the SnO_2 layer (working electrode) and the potentiostat. The cell along with all unshielded connecting

Table III. Cyclic Voltammetry Parameters for Reversible or Quasi-Reversible Redox Reactions of Metal Complexes of mnt at a Pt Electrode in MeCN

complex	$E_{1/2}$,[a]/V			ΔE/V		
	$0 \rightleftharpoons 1-$	$1- \rightleftharpoons 2-$	$2- \rightleftharpoons 3-$	0/1-	1-/2-	2-/3-
Ni(mnt)$_2^n$	+0.82[b]	-0.14	-1.94[c]		0.13	
Cu(mnt)$_2^n$	+0.96[b]	-0.03	-1.07		0.06	0.10
Pd(mnt)$_2^n$	+0.48	+0.04	-2.17[c]	0.38	0.16	
Pt(mnt)$_2^n$	+0.72	-0.16	-2.68[d] -2.97[d]	0.07	0.07	

[a] Potential measured halfway between peak anodic and cathodic potentials at a scan rateof 100 mV/s. [b] Irreversible in CH_3CN at Pt; the potential mentioned is the peak anodic potential. [c] Value taken from ref 14 and 15 corrected to Ag/Ag^+ redox couple. [d] See ref 14 and 15 for explanation.

Table IV. Cyclic Voltammetry Parameters for Reversible or Quasi-Reversible Redox Reactions of Metal Complexes of mnt at an SnO_2 Electrode in MeCN

complex	$E_{1/2}$[a]/V			ΔE/V		
	$0 \rightleftharpoons 1-$	$1- \rightleftharpoons 2-$	$2- \rightleftharpoons 3-$	0/1-	1-/2-	2-/3-
Ni(mnt)$_2^n$	*a*	-0.11	*b*		0.45	*b*
Cu(mnt)$_2^n$	*b*	+0.015	-1.17		0.40	0.49
Pd(mnt)$_2^n$	+1.11[c]	-0.02	*b*	0.90	1.03	*b*
Pt(mnt)$_2^n$	+1.13	-0.13	*b*		0.39	*b*

[a] See corresponding footnotes to Table III. [b] See text for explanation. [c] Irreversible in CH_2CN at SnO_2 electrode; the potential mentioned is E_{pa}, the anodic peak potential.

ends of the potentiostat was enclosed in a Faraday cage to reduce the electrical noise.

Spectrograde acetonitrile (American Chemicals) was kept under an inert atmosphere. Anhydrous sodium perchlorate (Anachemia) was stored under vacuum at 200 °C. Solutions for photoelectrochemical measurements were made by pumping the acetonitrile solvent directly into a reservoir containing sodium perchlorate, which served as inert electrolyte (0.1 M), and the maleonitriledithiolate complex. The solution was circulated at the rate of 45 mL/min from the closed reservoir with use of a Masterflex peristaltic pump and silicone tubing. The reservoir was equipped for deaeration of the solution by means of a glass frit dispersion tube. Deoxygenation was presumed to be accomplished after continuous passage of a stream of purified nitrogen gas for 2 h.

A supply of dry oxygen-free nitrogen was obtained by passing prepurified nitrogen through columns of 4A molecular sieves and supported copper catalyst, a system described in the literature.[11] The catalyst was prepared by the method of Meyer and Ronge[12] on a Diatomite support.

The solution was irradiated through the SnO_2 electrode with either an Ar ion Laser (nominally 6 W) from Coherent Radiation or a 200-W xenon lamp filtered by 6 cm of water and a 420 nm cutoff filter to eliminate IR and UV radiation, respectively. The light beam was interrupted at a frequency of 13 Hz by a Model CA chopper from Hurst Manufacturing Corp. The output level of the chopped beam was monitored at the front face of the SnO_2 electrode by a Coherent Radiation power meter that had been calibrated by Reineckate chemical actinometry.[13] A small portion of the beam was deflected by a beam splitter to a photodiode, which served as a reference channel signal for a PAR Model 128 lock-in amplifier. The lock-in amplifier received its input from the current channel of the potentiostat, and its output was recorded on a strip-chart recorder. The phase relation between the output of the lock-in amplifier and the irradiation beam was determined with use of an input signal from a photodetector positioned in the place of the photoelectrochemical cell.

Results

Electrochemical Behavior of [$M(S_4C_4CN)_4$] (M = Ni, Cu, Pd, Pt) at an SnO_2 Electrode. Since the photoelectrochemical measurements are at SnO_2, the electrochemical behavior of the above complexes at this electrode was examined by cyclic voltammetry. The redox processes were characterized by comparison with the known reactions[14,15] occurring at a Pt electrode. The voltammetric parameters at Pt and SnO_2 electrodes are presented in Tables III and IV, respectively.

The shapes of the current-potential curves for $M(mnt)_2^{2-}$/$M(mnt)_2^-$, where M = Ni, Cu, Pt, at the SnO_2 electrode are symmetrical and well developed but are unlike those at the Pt electrode in that they are broader. The ΔE_p (the anodic and cathodic peak separation) at the SnO_2 electrode is larger than that obtained for the same scan speed at the Pt electrode. The larger ΔE_p usually indicates slower heterogeneous electron transfer. The waves corresponding to the oxidation of $Ni(mnt)_2^-$ and $Cu(mnt)_2^-$ at the SnO_2 electrode are not resolved; instead, they appeared to be very much diffused and merged with the background current of the electrolyte. The voltammograms of $Cu(mnt)_2^n$ are shown in

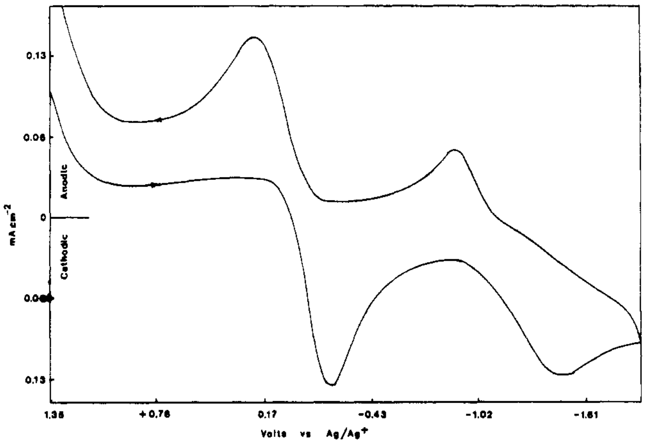

Figure 1. Cyclic voltammogram of $Cu(mnt)_2^{2-}$ at an SnO_2 electrode in 0.1 M $NaClO_4/CH_3CN$ solution (scan rate 100 mV s^{-1}).

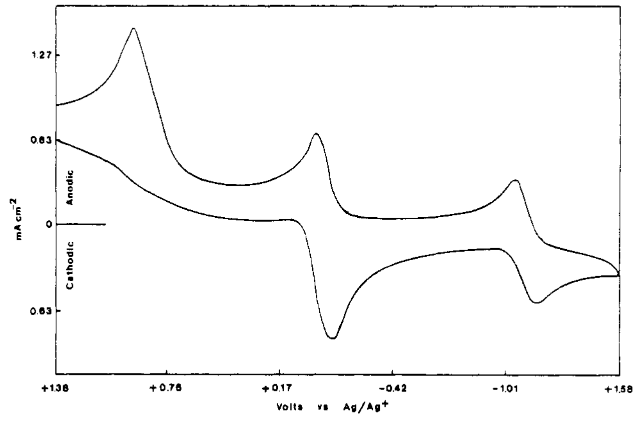

Figure 2. Cyclic voltammogram of $Cu(mnt)_2^{2-}$ at a Pt electrode in 0.1 M $NaClO_4/CH_3CN$ solution (scan rate 100 mV s^{-1}).

---

(11) D. T. Sawyer and J. L. Roberts, Jr., "Experimental Electrochemistry for Chemists" Interscience, New York, 1974.

(12) F. R. Meyer and G. Ronge, *Angew. Chem.*, **52**, 637 (1939).

(13) C. H. Langford and H. Kido, *J. Am. Chem. Soc.*, **105**, 1196 (1983).

(14) F. C. Senftleber and W. E. Geiger, *J. Am. Chem. Soc.*, **97**, 5018 (1975).

(15) T. E. Mines and W. E. Geiger, Jr., *Inorg. Chem.*, **12**, 1191 (1973).

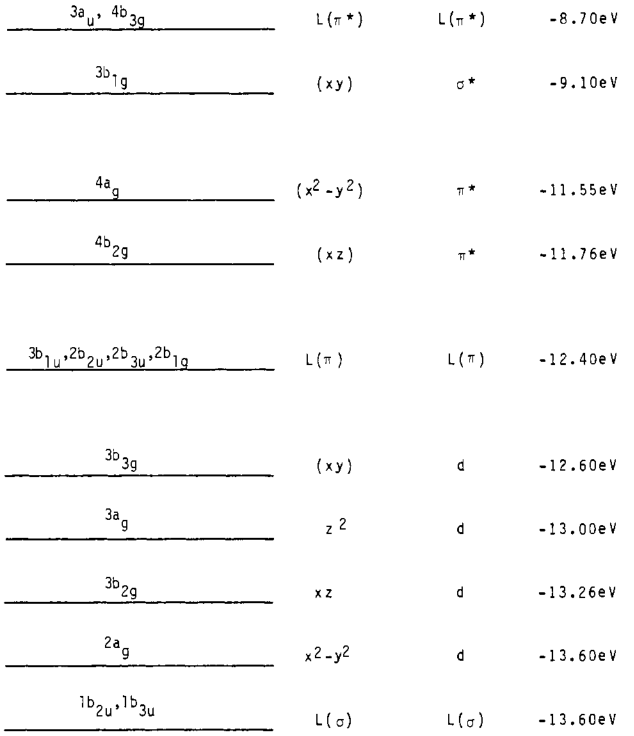

$3a_u$, $4b_{3g}$	L(π*)	L(π*)	-8.70eV
$3b_{1g}$	(xy)	σ*	-9.10eV
$4a_g$	(x^2-y^2)	π*	-11.55eV
$4b_{2g}$	(xz)	π*	-11.76eV
$3b_{1u}$,$2b_{2u}$,$2b_{3u}$,$2b_{1g}$	L(π)	L(π)	-12.40eV
$3b_{3g}$	(xy)	d	-12.60eV
$3a_g$	z^2	d	-13.00eV
$3b_{2g}$	xz	d	-13.26eV
$2a_g$	x^2-y^2	d	-13.60eV
$1b_{2u}$,$1b_{3u}$	L(σ)	L(σ)	-13.60eV

Figure 3. Simple MO scheme of $Ni(mnt)_2^{2-}$ as prepared by Gray et al.[7]

Figures 1 and 2. The reduction of $Cu(mnt)_2^{2-}$ to the trianion and the oxidation of monoanion to the neutral species have not been reported before. The wave at +0.71 V in Figure 2 is assigned as the oxidation reaction of the monoanion. It falls in the potential range for the oxidation of $Ni(mnt)_2^-$. This is because the oxidation process of the monoanion results in the removal of an electron from a primarily ligand-based orbital, rendering the oxidation practically independent of the identity of the metal. The reversible wave at -1.07 V (Figure 2) is assigned to the $Cu(mnt)_2^{2-}/Cu(mnt)_2^{3-}$ redox reaction. This potential is approximately 1.0 V more anodic for the analogous process of the nickel complex. A d^9 formulation can be considered for the metal ion in the $Cu(mnt)_2^{2-}$ complex, which makes it isoelectronic with the trianion of nickel. The degree of metal contribution to the HOMO, $3b_{1g}$, is expected to be similar for $Ni(mnt)_2^{3-}$ and the dianion of copper. Thus, the reaction is a more metal-centered reduction.

Similarly to Ni, the redox process of $Pt(mnt)_2^-/Pt(mnt)_2^0$ was found to be irreversible at Pt and SnO_2 electrodes in acetonitrile. The reversibility of this reaction is dependent on the solvent since it was found to be reversible in dichloromethane.[14,15] The wave associated with this anodic reaction at the SnO_2 electrode in acetonitrile is broad and diffuse.

The $Pd(mnt)_2^n$ complexes show quasi-reversible reaction for the processes $Pd(mnt)_2^0/Pd(mnt)_2^-$ and $Pd(mnt)_2^-/Pd(mnt)_2^{2-}$ at the SnO_2 electrode.

Electronic Absorption Spectra. The electronic absorption spectra of these complexes have been previously assigned. Two important approaches have been reported in Table I. The assignments by Gray and his co-workers[7] were based on MO calculations for $Ni(mnt)_2^{2-}$; those of Schrauzer and Mayweg[16] are based on calculations on the neutral complex $NiS_4C_4(C_6H_5)_4$. Since our purpose is to relate the assignments to photochemical results and not the adjudication of spectroscopic fine points, we follow the Gray assignment without detailed comment. This choice is because these assignments are based on one of our anionic complexes. Schrauzer and Mayweg[16] observe that the neutral species is rather different. We will also see below that there is also a photochemical precedent favoring these assignments. The assignments in Table II that are new are based on Gray's work.

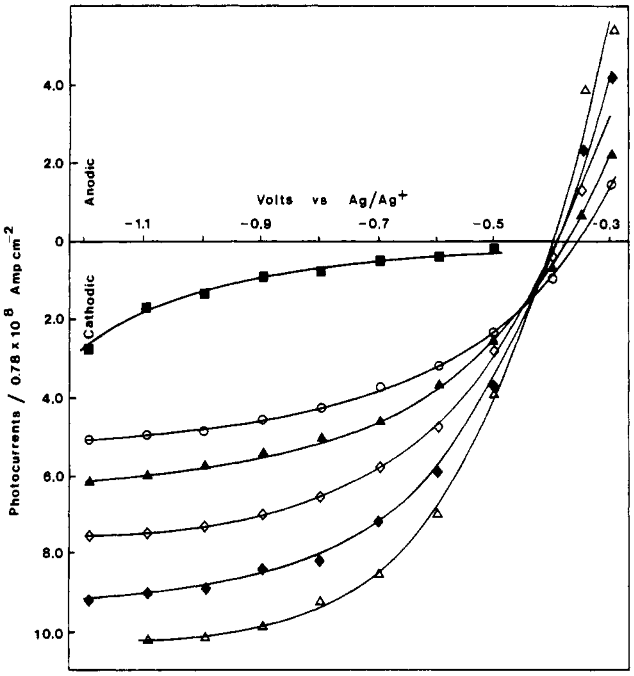

Figure 4. Dependence of photocurrent on potential and concentration of $Ni(mnt)_2^{2-}$ in 0.1 M $NaClO_4/CH_3CN$ electrolyte. $Ni(mnt)_2^{2-}$ concentration: (■) 0; (○) 2 × 10^{-3} M; (▲) 4 × 10^{-3} M; (◇) 6 × 10^{-3} M; (◆) 8 × 10^{-3} M; (△) 1 × 10^{-2} M. The irradiation source was an argon ion laser in multimode (200 mW).

A representative MO diagram is shown in Figure 3.

Photoelectrochemical Measurements. The experimental arrangement in these investigations was introduced by Phillips et al.[4,17] It requires irradiation of the solution through the optical electrode to generate excited states in the solution but close to the electrode so that these species can diffuse and react at the electrode within their excited-state relaxation time. The continuous circulation of the electrolytic solution through the cell suppressed thermally induced current resulting from light absorption, replenished the electrode surface with the reactant, and simultaneously flushed any photoinduced reaction products that may tend to be adsorbed on the electrode. This technique has proven successful in detecting short-lived excited-state species and estimating their lifetimes from kinetics of competing reactions. The capacity to estimate short lifetimes can be appraised by referring to earlier works[17] in which an excited-state lifetime in the nanosecond domain was determined for the nonluminescent $Fe(bpy)_3^{2+}$.

Two preliminary observations concerning the present compounds may be made. Despite the strong absorbance of all compounds, not all produced photocurrents and the currents that were observed were generally in the nanoampere domain.

Moreover, the phase relation data obtained with the lock-in amplifier indicated that the photocurrents were in phase with the chopper (contrast reports of sensitized $Fe(bpy)_3^{2+}$ currents[17]). These features suggest direct reaction of short-lived excited states at the transparent electrode. The possibility that "photocurrents" are dominantly thermal is eliminated by the fact that their magnitude was independent of the "duty cycle" of the chopper and that they frequently had signs opposite that of background current. However, it is clear from blank runs that "thermal" effects of light become significant in potential regions where background currents are large. This is as expected.

Figure 4 shows the dependence of photocurrent for solutions prepared from $Ni(mnt)_2^{2-}$ as a function of potential and complex concentrations. The photowave between -0.5 and -1.0 V is in

---

(16) G. N. Schrauzer and V. P. Mayweg, *J. Am. Chem. Soc.*, **87**, 3585 (1965).

(17) J. Phillips, C. H. Langford, J. A. Koningstein, and R. Sasseville, *J. Phys. Chem.*, **82**, 622 (1978).

(18) J. A. McCleverty, *Prog. Inorg. Chem.*, **10**, 49 (1968).

(19) H. B. Gray, R. Williams, E. Billing, and J. H. Walters, *J. Am. Chem. Soc.*, **88**, 43, 1966.

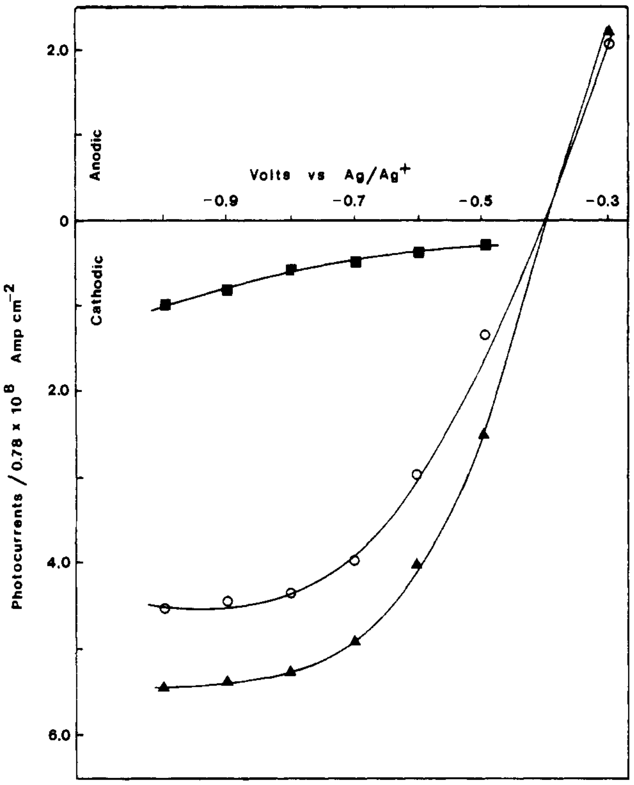

Figure 5. Dependence of photocurrent on potential and concentration of $Pt(mnt)_2^{2-}$ in 0.1 M $NaClO_4/CH_3CN$ electrolyte. $Pt(mnt)_2^{2-}$ concentration: (■) 0; (○) 2×10^{-3} M; (▲) 4×10^{-3} M. The irradiation source was a xenon lamp with IR and UV cutoff filters (100 mW).

a region where background currents are small enough to allow accurate observations. The height of the wave is approximately linearly related to concentration. It is also proportional to approximately the first power of the laser intensity. A similar wave is observed for solutions prepared from $Pt(mnt)_2^{2-}$. This is shown in Figure 5. No similar wave was recorded for $Pd(mnt)_2^{2-}$ solutions.

The limited potential regions of small enough background current to permit exploration of photocurrents do not allow the examination of all oxidation states of the complexes, but in the region where $Ni(mnt)_2^-$ is stable, an anodic photocurrent is detectable. This is shown in Figure 6. The "wave" is not defined because the limiting current is reached above +0.7 V, where background currents become large; thus it is difficult to specify a detailed mechanism. Finally, $Cu(mnt)_2^{2-}$ solutions (Figure 7) do not show important photocurrents in the 2– oxidation state range, but at potentials sufficiently cathodic for $Cu(mnt)_2^{3-}$ to be an important species at the electrode, anodic photocurrents arise. We suggest direct oxidation of the 3– species which is formally Cu(I).

The photocurrents seen for $Ni(mnt)_2^{2-}$, $Pt(mnt)_2^{2-}$, and $Cu(mnt)_2^{3-}$ are at least partially quenched by O_2; typically air-saturated currents are only about 60% of those in air-free solutions. This may not be of direct significance for $Cu(mnt)_2^{3-}$ since the O_2 may reoxidize the trianion itself, but it seems significant in the other cases. Additionally, pyridine quenches $Ni(mnt)_2^{2-}$ photoelectrochemistry. The quenching is partial and does not follows Stern–Volmer behavior accurately. A plot in Stern–Volmer form is shown in Figure 8.

Approximate photoelectrochemical "half-wave" potentials at -0.6 ± 0.1 V can be discerned for $Ni(mnt)_2^{2-}$ and $Pt(mnt)_2^{2-}$. These values fit to assignment of the reduction of the excited state produced by absorption in the visible band assigned as M → $L\pi^*$ by Gray et al. For example, in the Ni case, the standard potential for the 2–/3– couple is –1.9 V at Pt. The excitation energy for the first excited state is 1.4 eV. The difference yields approximately –0.5 V for a predicted *2–/3– couple, where the asterisk designates the excited states. The corresponding quantities for the Pt complex are –3.0 V and 2.3 eV, yielding approximately –0.7 V for *2–/3–.

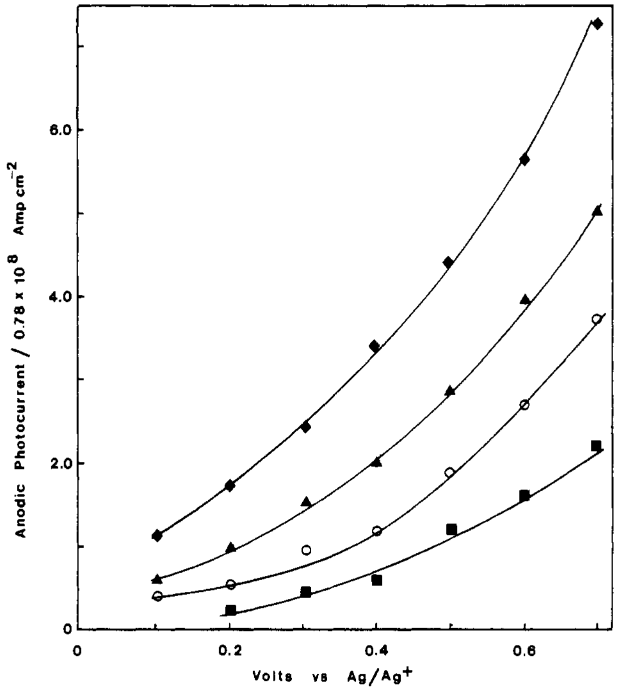

Figure 6. Dependence of photocurrent on potential and concentration of $Ni(mnt)_2^-$ in 0.1 M $NaClO_4/CH_3CN$ electrolyte. $Ni(mnt)_2^-$ concentration: (■) 0; (○) 2×10^{-3} M; (▲) 4×10^{-3} M; (♦) 8×10^{-3} M. The irradiation source was an argon ion laser in multimode (200 mW).

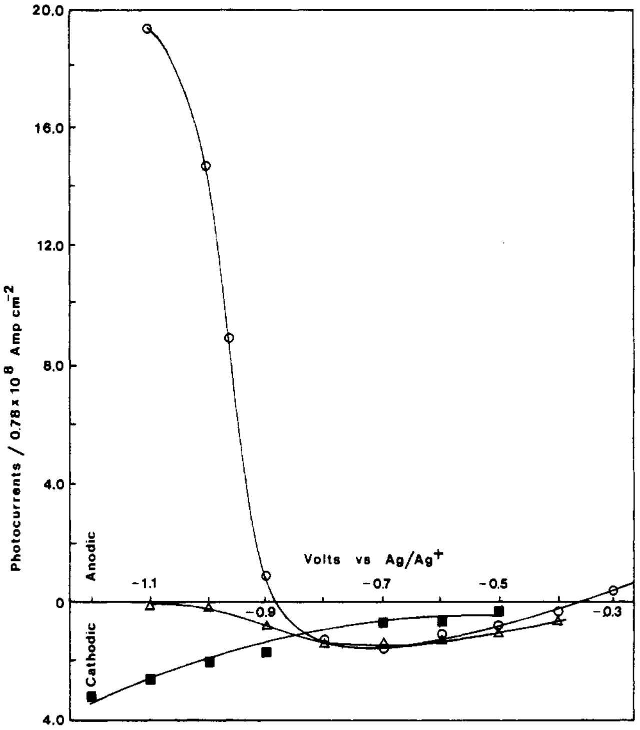

Figure 7. Effect of potential and oxygen on photocurrents of $Cu(mnt)_2^{2-}$ in 0.1 M $NaClO_4/CH_3CN$ electrolyte: (■) electrolyte saturated with O_2 gas; (△) 2×10^{-3} M $Cu(mnt)_2^{2-}$ in electrolyte saturated with O_2 gas; (○) 2×10^{-3} M $Cu(mnt)_2^{2-}$ in electrolyte. The irradiation source was an argon ion laser in multimode (200 mW).

Discussion

The first pattern of photochemistry reported here, $Ni(mnt)_2^{2-}$ being similar to $Pt(mnt)_2^{2-}$ but different from $Pd(mnt)_2^{2-}$, is precisely that reported by Dooley and Patterson[3] for initiation of oxidation of halocarbon solvents. In that case, the pattern was attributed to excitation of a character $L\pi$ → $L\pi^*$ (L = ligand)

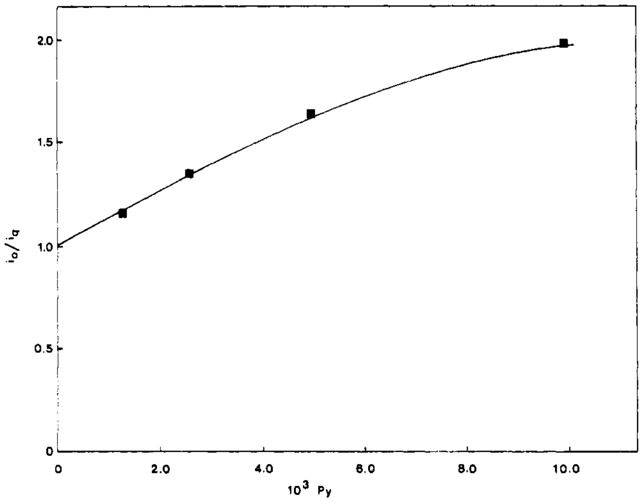

Figure 8. Stern–Volmer plot for quenching of $Ni(mnt)_2^{2-}$ photocurrents by pyridine. The irradiation source was a xenon lamp with IR and UV cutoff filters (100 mW).

because of the action spectrum and it was observed that this transition decreases bonding electron density at the metal. In the present case, the assignments of Gray et al.[7] indicate that the cathodic photocurrents are observed in complexes where the transition dominating the excitation region is of M → Lπ*. The main visible band of the Pd complex is L → M. We suggest that the cathodic photocurrents reflect electron capture by a vacated HOMO of largely metal character and that Pd complexes are the exceptions spectroscopically and photoelectrochemically.

If this assignment is correct, it implies an interpretation of the difference between the Ni and Pt complexes and the Cu complex. The $Cu(mnt)_2^{2-}$ complex exhibits a M → Lπ* transition also, but as an odd-electron system, the transitions are all doublet–doublet. In the case of the Ni and Pt complexes, an intersystem crossing is possible and a triplet state of potentially longer lifetime could intervene.

The above speculative assignments require short-time-scale photophysical studies as a test. Such studies have been initiated with use of the facilities of the Canadian Centre for Picosecond Laser Flash Photolysis and will be reported elsewhere.[20] We note that short-lived excited-state signals are observable in the form of bleaching of absorbance at the maximum which recovers. A transient to the red of the maximum in $Pt(mnt)_2^{2-}$ may be the required triplet.

It is possible to use consideration of competitive kinetics to estimate the lifetime domain of species generating photocurrents. $Ni(mnt)_2^{2-}$ is a representative case. The relevant mechanism is

$$\begin{aligned} &\mathrm{Ni(mnt)_2^{2-}} \underset{k_{-1}}{\overset{k(h\nu)}{\rightleftharpoons}} \mathrm{{}^*Ni(mnt)_2^{2-}} \\ &\mathrm{{}^*Ni(mnt)_2^{2-}} \xrightarrow{k_2} \mathrm{Ni(mnt)_2^{3-}} \\ &\mathrm{Ni(mnt)_2^{3-}} \xrightarrow{k_3} \mathrm{Ni(mnt)_2^{2-}} \end{aligned} \qquad (1)$$

where the asterisk denotes an excited state. k_2 and k_3 represent rate constants for reduction of the excited state and reoxidation of the ground-state product. The latter reaction is favorable with an overpotential of up to a few hundred millivolts in the region of the tip of the "photowave" (see Figure 4). The overvoltage driving the k_2 process is large in the limiting region of the "photowave". Since a limiting region is established, we assign $k_2 > k_3$ in that region. The steady-state equation for the excited state is (2), where ϕ is the quantum yield for formation of the

$$\mathrm{d[{}^*Ni(mnt)^{2-}]}/\mathrm{d}t = \phi I\xi[\mathrm{Ni(mnt)_2^{2-}}] - k_{-1}[\mathrm{{}^*Ni(mnt)_2^{2-}}] - k_2[\mathrm{{}^*Ni(mnt)_2^{2-}}] \qquad (2)$$

reactive excited state, I is the light intensity, and ξ is the average extinction coefficient between 450 and 570 nm. If we solve (2)

$$[\mathrm{{}^*Ni(mnt)_2^{2-}}] = \phi I\xi[\mathrm{Ni(mnt)_2^{2-}}]/(k_{-1} + k_2) \qquad (3)$$

where ϕ will be aproximated as unity, I is 1.2×10^7 einsteins s^{-1}, and ξ is approximately 5.6×10^3 M^{-1} cm^{-1}.

Now the limiting current is given by

$$i_1 = nFA \qquad (4)$$

(flux of excited state to electrode), where n is the number of electrons, F is the Faraday constant, and A is the area of the electrode. The flux of the excited state to the electrode is given by

$$\text{flux} = D[\mathrm{{}^*Ni(mnt)_2^{2-}}]/\delta \qquad (5)$$

where δ is the thickness of the diffusion layer. If the diffusion layer is thicker than the distance traveled by an excited state in its lifetime, it will not contribute to the current. Thus, we take $\delta = (D\tau)^{1/2}$, where D is the conventional diffusion coefficient of approximately 1×10^{-5} cm^2 s^{-2} and τ is the excited-state lifetime, $1/k_{-1}$. Collecting all terms and assuming $k_{-1} > k_2$ yields

$$i_{lm} = \frac{nFAD\phi I\xi[\mathrm{Ni(mnt)_2^{2-}}]}{D^{1/2}k_{-1}{}^{1/2}} \qquad (6)$$

The average value of k_{-1} from (6) for the concentration range studied is 2.5×10^8 s^{-1}. The corresponding lifetime is approximately 4 ns.

There are two major limitations on this analysis. If $\phi < 1$, then k_{-1} can be less and the lifetime longer. Conversely, if there is specific adsorption of the complex at the electrode, the simple diffusion model unerestimates delivery of excited states and the lifetime may be shorter. The failure of the pyridine quenching data to fit accurately to a Stern–Volmer plot suggests some specific adsorption. An analysis similar to that given for Ni yields a lifetime of 43 ns for the $Pt(mnt)_2^{2-}$ complex.

Conclusion

The observed photocurrents for visible irradiation of the complexes are rather small and appear to be limited to those cases where a M → Lπ* state is available and intersystem crossing to a state separated from the ground state by a spin-forbidden process is possible. This suggests generally rapid return to ground states, and analysis of competition with diffusion does yield rather short lifetimes. Probably the reason follows from the energy gap law. The lowest lying excited states are relatively close to the ground state. If these states are to be used in "applied" photoelectrochemistry, the lifetimes need to be extended. Attachment to a solid surface may prove profitable.

Registry No. $Ni(mnt)_2^{2-}$, 14876-79-0; $Cu(mnt)_2^{2-}$, 19562-26-6; $Pd(mnt)_2^{2-}$, 19555-33-0; $Pt(mnt)_2^{2-}$, 15152-99-5; $Ni(mnt)_2^{-}$, 46761-25-5; $Cu(mnt)_2^{-}$, 14432-31-6; $Pd(mnt)_2^{-}$, 19570-29-7; $Pt(mnt)_2^{-}$, 14977-45-8; $Ni(mnt)_2$, 19280-13-8; $Cu(mnt)_2$, 97973-45-0; $Pd(mnt)_2$, 56644-13-4; $Pt(mnt)_2$, 56644-14-5; $Cu(mnt)_2^{3-}$, 77089-70-4; $[(C_2H_5)_4N]_2[Ni(mnt)_2]$, 15665-90-4; $[(C_2H_5)_4N]_2[Cu(mnt)_2]$, 15744-45-3; $[(C_2H_5)_4N]_2[Pd(mnt)_2]$, 15665-98-2; $[(C_2H_5)_4N][Ni(mnt)_2]$, 39008-57-6; $[(C_2H_5)_4N][Pd(mnt)_2]$, 21328-88-1; $[(C_2H_5)_4N][Cu(mnt)_2]$, 15711-72-5; $[(C_2H_5)_4N]_2[Pt(mnt)_2]$, 15711-73-6; SnO_2, 18282-10-5; Pt, 7440-06-4.

---

[20] L. Persaud, C. H. Langford, and D. K. Sharma, to be submitted for publication.